NASA TECHNICAL NOTE

NASA TN D-1841

NASA TN D-1841

CHARACTERISTIC OF PASSIVE COMMUNICATION SATELLITES WITH LAMBERTIAN SURFACES

by Herbert P. Raabe;
General Mills Electronics Division,
Minneapolis, Minnesota

NATIONAL AERONAUTICS AND SPACE ADMINISTRATION - WASHINGTON, D. C. - SEPTEMBER 1963

TECHNICAL NOTE D-1841

CHARACTERISTICS OF PASSIVE COMMUNICATION SATELLITES WITH LAMBERTIAN SURFACES

By Herbert P. Raabe

General Mills Electronics Division
Minneapolis, Minnesota

NATIONAL AERONAUTICS AND SPACE ADMINISTRATION

CHARACTERISTICS OF PASSIVE COMMUNICATION SATELLITES WITH LAMBERTIAN SURFACES

by
Herbert P. Raabe
General Mills Electronics Division

SUMMARY

Passive Communication Satellites with surfaces reflecting diffusely according to Lambert's law are particularly attractive since they afford a directional pattern well matched to the optimum pattern of satellites in lower orbits and since such surfaces are easily realized. The echo from diffuse reflectors varies statistically, and a combination diversity technique of frequency should be used to stabilize the signal. A spherical satellite is no longer required; and weight reduction and higher reliability can be gained from polyhedral structures. Compared with a rigidized specularly reflecting sphere, a Lambertian reflector affords a 7 db stronger echo for the same weight. Model tests of reflectivity agree well with the theory.

CONTENTS

CHARACTERISTICS OF PASSIVE COMMUNICATION SATELLITES WITH LAMBERTIAN SURFACES*

by
Herbert P. Raabe
General Mills Electronics Division

INTRODUCTION

The most attractive characteristic of passive communication satellites is their long lifetime. Other advantages are unlimited linearity and very broad bandwidth. Their major disadvantage, however, is their low ratio of radiant intensity to weight as compared with that of active satellites. The passive satellites must be very large to intercept sufficient electromagnetic radiation power for retransmission toward the earth, in contrast to active satellites which amplify the signal enormously. Actually, a very small amount of metal is required to intercept the electromagnetic energy over the cross section of a passive satellite. Most of its weight is required to provide strength and rigidity and to package and erect the satellite. The weight of Echo I (1960 ι) is about one thousand times that of the theoretical minimum. This shows that there is a great need for improved satellite construction techniques.

To maximize the ratio of radiant intensity to weight—or the effectiveness of the passive satellite—not only should the intercepting cross section be increased or the weight decreased, but also the reflected power should be concentrated into the smallest solid angle consistent with the geometry of the desired propagation paths. Moreover, within this solid angle there is an optimum distribution of radiant intensity when various locations of terminals and their relations to the orbital position of the satellite are considered. Since a specularly reflecting sphere is an isotropic scatterer, the gain of a directional reflection or scattering pattern indicates the gain in radiant intensity over that of a perfect sphere having the same intercepting cross section as the modified satellite. Obviously, since the useful maximum gain is a function of orbital height, different approaches must be taken for synchronous satellites and for those in lower orbits. This paper discusses only satellites in the 2,000 to 5,000 km altitude range. The study of such satellites, partially supported by the U. S. Navy Contract Nonr (3545) (00) (X), showed that the theoretically achievable gain is not very high, so that parallel efforts to reduce the weight become more important. Attitude control of the satellites was, therefore, ruled out as an unacceptable complexity. Schemes utilizing refraction were also rejected because dielectric materials—even artificial ones—would be too heavy, and the problem of erection in space too difficult. Thus only one approach to a solution for the problem could be found, namely, an

*Presented at the XIII International Astronautical Congress, Varna, Bulgaria, September 28, 1962. This work was performed under contracts NAS5-890 and NAS 5-1598 for the Goddard Space Flight Center.

approximately spherical array of scatterers with more or less directive characteristics. As these scatterers reradiate waves of random phases, such a satellite becomes a diffuse reflector. Its scattering characteristic is always axially symmetric with respect to the direction of the transmitter.

THE OPTIMUM SCATTERING CHARACTERISTIC

Whenever the satellite is in a favorable position for communication between two terminals, the received power should exceed a maximized threshold. The received power is determined by

$$P_r = \frac{P_t G_t}{4\pi s_t^2} \frac{AG_\psi}{4\pi} \frac{G_r \lambda^2}{4\pi s_r^2} , \tag{1}$$

where

P_t = transmitted power,

G_t = gain of transmitting antenna,

G_r = gain of receiving antenna,

λ = wavelength,

A = intercepting area of the satellite,

G_ψ = gain of the satellite (pattern),

ψ = bistatic angle,

s_t = satellite distance from the transmitter,

s_r = satellite distance from the receiver.

The first term of Equation 1 defines the irradiance in the vicinity of the satellite, while the first two terms determine the radiant intensity of the satellite. As a comprehensive term we define the bistatic scatter cross section as

$$\sigma_\psi = A G_\psi . \tag{2}$$

Of particular interest is the factor

$$\alpha = \frac{\sigma_\psi}{s_t^2 s_r^2} , \tag{3}$$

which consists of those parameters characteristic of the satellite and its orbital position. Figure 1 illustrates, in a general manner, the geometry of the triangle formed by the terminals and the satellite.

The transmitter has been assumed to be at T and the receiver is at R. The satellite S may be found anywhere in the orbital shell, but it becomes operational as a communication link only during passage through the segment which is visible from both terminals. The ranges s_t and s_r and the bistatic angle ψ vary in a complicated manner, but one significant fact is obvious: larger angles are associated with shorter ranges.

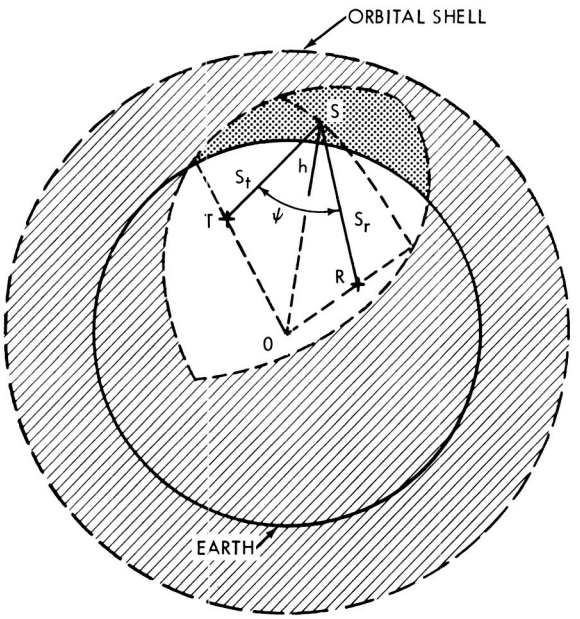

Figure 1—Geometry of the propagation path.

For a realistic case, some characteristic ranges and angles have been determined as shown in Figure 2. The terminals are located at New York (NY) and Paris (P), while the satellite may be found in orbits between 2400 and 4000 km above the earth. Positions S_1 and S_2 correspond to the lowest and highest orbit respectively, while S′ is in the center of the operational segment, S″ in the center of the arcs, and S‴ at the intersection of the arcs. The true bistatic angles at S‴ are illustrated in the "tilted-up" triangles. The correlation between angles and ranges is clearly indicated, so that the optimum pattern should be a broad lobe with a gradual dropoff toward larger angles.

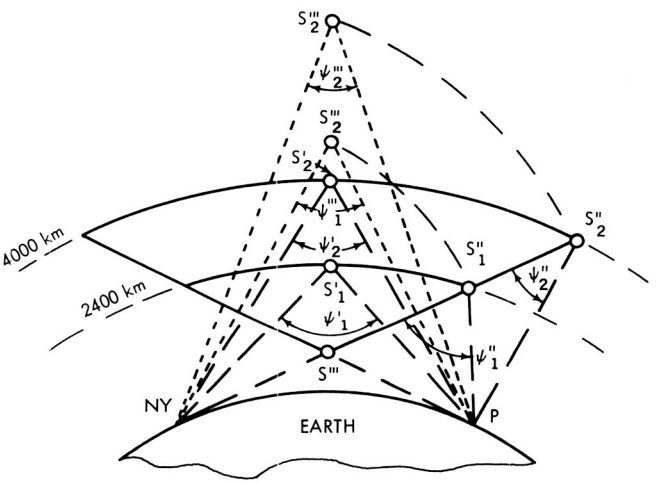

Figure 2—Geometry of a satellite communication case.

THE SPHERICAL LAMBERTIAN SURFACE

Under certain conditions, a surface scatters incident electromagnetic radiation diffusely according to Lambert's cosine law. A spherical satellite with a Lambertian surface proved to be particularly useful because its scattering characteristic matches the optimum pattern rather closely, and Lambert's law applied to certain randomly distributed surfaces which greatly ease design specifications.

For a spherical Lambertian surface the bistatic scattering cross section can be derived as follows: A plane surface element whose normal is inclined toward the direction of the incident radiation at an angle β intercepts the power

$$dP_i = H ds \cos \beta \qquad (4)$$

from the homogeneous radiation field of the irradiance H. If the albedo of this Lambertian surface element is a, the radiant intensity of the scattered radiation is described by

$$dJ_s = \frac{aHds}{\pi} \cos\beta \cos\phi \ , \tag{5}$$

where ϕ is the angle between the normal of this surface element and the observer. The term $\cos\phi$ is characteristic of Lambert's law, and means that the radiance of a plane surface is independent of the angle ϕ of the observer since the projected area in the direction of the observer also varies as $\cos\phi$.

If ds is a surface element on a Lambertian sphere of radius r, the radiant intensity can be derived by integration over the visible irradiated section of the surface:

$$J_s = aH\frac{2r^2}{3\pi} \left[\sin\psi + (\pi - \psi)\cos\psi\right] \tag{6}$$

We can use Equation 3 to determine the bistatic scattering cross section of the Lambertian sphere and, with $a = 1$, we obtain

$$\sigma_L = \frac{8r^2}{3} \left[\sin\psi + (\pi - \psi)\cos\psi\right] \tag{7}$$

However, the isotropic scattering by a specularly reflecting sphere is simply

$$\sigma_S = r^2\pi \ . \tag{8}$$

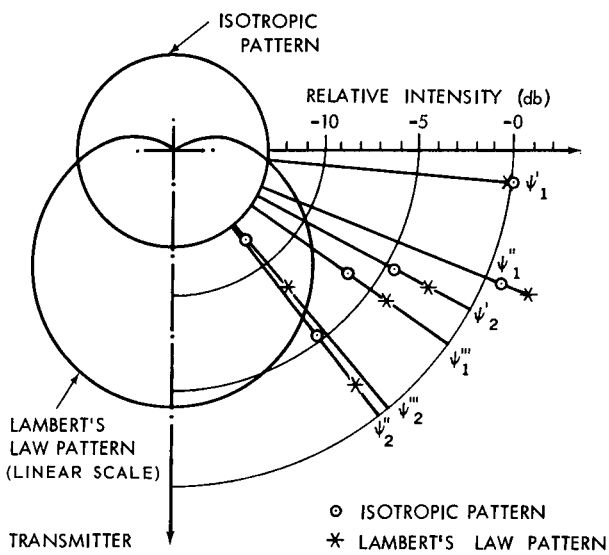

Figure 3—Isotropic and Lambertian patterns and relative signal strengths for Figure 2.

These two patterns are shown in Figure 3. The maximum gain of the diffuse sphere over the specular sphere is 2.67 (4.3 db) in the direction of the transmitter. The gain tapers off gradually and reaches zero at an angle of 83.7 degrees.

To prove the suitability of the Lambertian pattern for non-synchronous satellites, the factor α (see Equation 3) was computed for the two patterns defined in Figure 2. The relative echo power level is plotted in Figure 3 for the bistatic angle designated. The Lambertian sphere is seen to afford a gain of 3 db to a system which must be designed to operate with the lowest level signal. Incidentally, at S'_1 the diffuse sphere is slightly less effective; but, because of the shorter ranges, the signal is still 8 db stronger than the least favorable position S''_2.

THE STATISTICAL PROPERTIES OF ECHO

Diffuse reflectors share one disadvantage with any scattering means of radio wave propagation. The echo does not appear to originate from a single phase center; it originates from a multitude of phase centers. Therefore, the power buildup is a statistical phenomenon, and the aforementioned scattering cross section is just the average of its statistical distribution. Moreover, the satellite is not stationary. As it revolves and travels along its orbit, the relative position (and hence the phase of the scatterers) changes. Consequently, a CW signal, or any spectral component of a signal, experiences a narrow-band noise modulation of phase and amplitude. Under the idealized assumption that the bistatic angle is zero and the satellite revolves about an axis which is perpendicular to the direction of the terminals, the situation illustrated in Figure 4 results. The lower half of the Lambertian sphere is illuminated and contributes to the echo. It is easy to show that the distribution of echo intensity with respect to the x axis is that of a parabola, as in the lower graph of Figure 4. Since the Doppler shift of the scattered radiation is proportional to x, the parabolic curve is also representative of the spectrum envelope.

The statistical distribution of a narrow-band noise voltage is Gaussian (Figure 5a). The envelope of the noise voltage follows the Rayleigh distribution. The intensity distribution of the noise signal (or the square-law rectified signal) follows the exponential curve shown in Figure 5b. These statistical variations can be very harmful to the transmitted signal. Special communication techniques can be applied, however, which result in very steady signals—a fact that is demonstrated by tropospheric scatter communication techniques. In principle, these techniques use a number of statistically independent samples for every bit of information. To get this independence, some diversity must be introduced. For example, if the satellite depolarizes the radiation completely, two

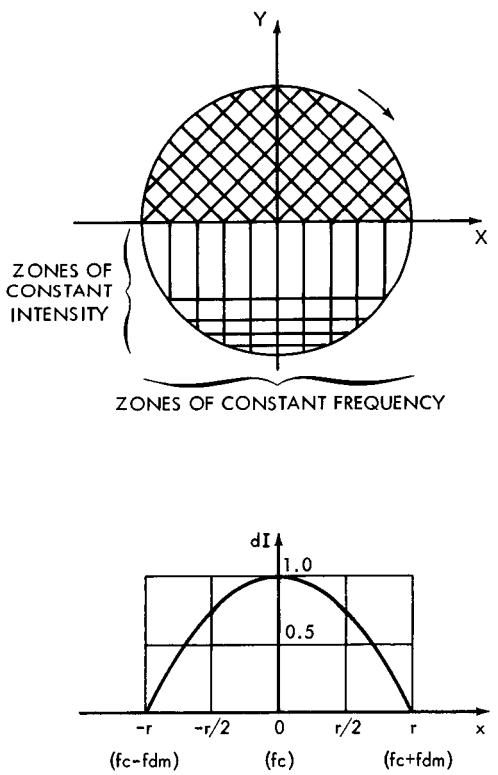

Figure 4—Intensity distribution and spectrum of a Lambertian sphere.

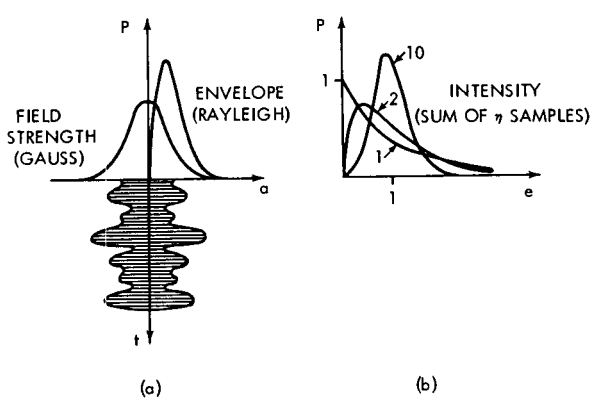

Figure 5—Statistical distribution functions of Echo I.

independent samples can be derived from the two orthogonal polarization channels. After rectification, the signals are added and the distribution of the sum follows curve 2 (figure 5b).

The preferred technique for tropospheric scatter propagation is space diversity. Independent samples can thus be obtained with several receiving antennas placed side by side. This is not practical for satellite scatter propagation because the receiving antennas have to be spaced several kilometers apart, and the cost would become excessive. Time diversity is also unattractive because of the low sample rate which is dependent upon the rotational rate of the satellite. Furthermore, satellite spin is somewhat unpredictable and decreases with age. The most attractive diversity technique is frequency diversity.

Just as the re-phasing of individual contributions of scattering centers causes signal fluctuation as the satellite revolves, re-phasing due to a variation of the frequency also causes signal fluctuation, and one would like to know how much the frequency must be shifted to obtain a decorrelated amplitude. As a simplified model, we assume two equally strong scattering centers whose path-length difference is 2b. Again, we assume that the two terminals are close together so that the separation in depth of the two scattering centers becomes b. Hence, a frequency can be chosen so that the contribution from both scatterers are in phase, resulting in a maximum amplitude. Then, a frequency shift to reduce the amplitude to zero would require the addition or subtraction of one-half wavelength within the delay path of 2b. To get an approximate figure for the required phase shift for full-size satellites, we assume that the illuminated side is divided into a near and a distant zone of equal reflectivity and that both zones are represented by a single scattering center. From Figure 4 one can estimate that the separation in depth of these centers is at least 1/8 of the diameter. For a 200-foot diameter satellite this separation is 25 feet (7.62 m) and the corresponding frequency shift is nearly 10 mc/s. Thus, several statistically independent samples can be derived from carriers of sufficient frequency separation for each bit of information. They may be transmitted coincidentally or sequentially.

The most efficient form of diversity technique is combination diversity, first introduced by Kahn (Reference 1) and more generally investigated by Brennan (Reference 2). This technique adds the n independent samples after weighing them according to their individual signal-to-noise ratios p_i and results in an overall signal-to-noise ratio of

$$P = \sum_{i=1}^{n} p_i \ . \tag{9}$$

Thus, the combination diversity technique can provide the same signal-to-noise ratio for a noncoherent scatter communication path as the standard technique achieves for the coherent scatter communication path with no additional demand in levels of power or sizes of antennas.

REALIZATION OF LAMBERTIAN SURFACES

The mechanism of scattering from rough surfaces that obey Lambert's law is not well understood. Although an abundance of literature exists which theoretically treats the scattering of electromagnetic

waves from rough surfaces, none was found where Lambert's law resulted. Most of the literature was generated with the intent of explaining scattering from the surface of the sea, which is not Lambertian. In this literature the surface is treated as a continuously illuminated or radiating boundary. Thus the effects of shadows and secondary scattering are not considered. Obviously, the sea never has a sufficiently rough surface to scatter radiation according to Lambert's law, so that simplifying assumptions are justified.

A rough surface may be treated as a random surface whose height over a smooth reference surface is defined as a continuous, single-valued statistical variable. The statistical parameters are constant over the entire reference surface. In application to satellites, this reference surface should be a sphere, but for general discussions it is assumed that the reference surface is a plane. As a further restriction only symmetrical, rough surfaces are considered, which means that the height of the surface has a symmetrical distribution about the first order mean; and for the sake of simplicity we assume that the reference surface is defined in such a way that this first order mean becomes zero.

For complete definition of the rough surface, we must specify the second probability distribution of height or the spatial frequency spectrum. These functions determine the roughness; thus we must differentiate between theoretical and effective roughness. Theoretical roughness is independent of the linear scale of the surface. However, since the rough surface is probed by electromagnetic radiation of limited resolving power, the effective roughness must take wavelength into account.

It was found that effective roughness is the theoretical roughness of a surface which has been smoothed to such a degree that its structure can be resolved by the radiation. This means that, if a surface is rough enough to achieve Lambertian scattering at a given frequency, Lambertian scattering will be assured for any higher frequency. It also means that smooth surfaces to which geometric optics apply can yet be rough enough to assure Lambertian scattering. Smoothing of a rough surface causes suppression of the higher spatial frequencies. Two point scatterers must be positioned at least one-half wavelength of the probing radiation apart to allow resolution. This means that, for the purpose of determining effective roughness, all components of the spatial frequency spectrum whose wavelengths are shorter than one-half of the radiated wavelength should be suppressed.

In order to determine the degree of roughness required to achieve Lambertian scattering, an experiment was performed on paper in which the surface was assumed smooth enough to obey laws of geometric optics. It consisted of a layer of reflective spheres whose radius was large compared to the wavelength of the illuminating radiation. To form a random rough surface, the heights of these spheres were statistically distributed, and then the scattering angles were traced for each sphere. The distribution was Gaussian and was varied in three steps of increasing standard deviation. Statistical data were obtained by the Monte Carlo method. The sample surface consisted of 20 spheres; three spheres are shown in Figure 6 to illustrate details of the ray tracing. The spheres were illuminated (normal to the reference plane) by a distant point source. The following simplifications and assumptions were considered justified: (1) The spheres are located in a vertical plane so that the problem can be treated as a two-dimensional one; (2) the image of the point source is in a fixed position halfway between the center and the surface of the sphere; and (3) only primary reflections

were traced. The result of this experiment is shown in Figure 7, where the distribution functions of the limiting angles (ϕ) are plotted for the standard deviations of 0, 0.2 r, 0.5 r, and r, where r is the radius of the spheres. All distribution curves were based on the same set of random two-digit numbers. The approach to a Lambertian distribution is evident, although twenty samples are a relatively small number with which to establish a statistical distribution.

As a measure of roughness for the array of spheres, we can use the ratio of the average slant distance between adjacent scattering centers to the distance between the spheres of a smooth array, which equals the diameter of the spheres. For the roughest array (σ = r), this ratio was found to be 1.28. Hence, the conclusion appeared to be justified that a randomly wrinkled reflective sheet whose surface is larger than the reference plane by a linear factor of 1.28 should perform as well as the respective array of spheres, provided the wrinkles are coarse enough to be resolved by the radiated wavelength. This led to a simple technique of generating rough surfaces: A sheet of aluminum foil was crumpled and reexpanded until the desired ratio of linear surface dimensions was reached. The pressure applied to the crumpled package of foil determined the range of the spatial frequency spectrum, but an allowance was made for some unresolvable wrinkles; and it was found that a linear surface ratio of 1.3 offered good agreement with Lambert's law.

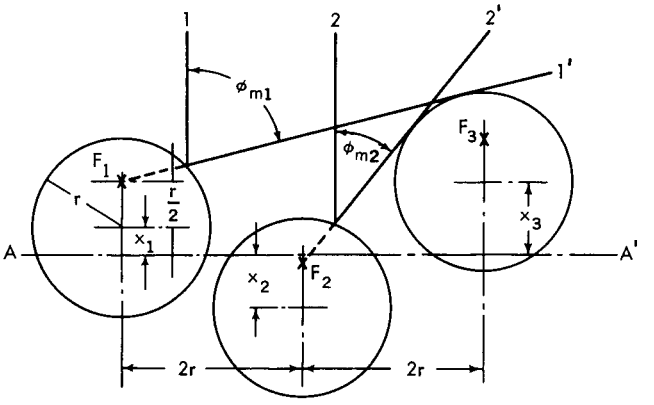

Figure 6—Geometry of limiting rays for randomly distributed spheres.

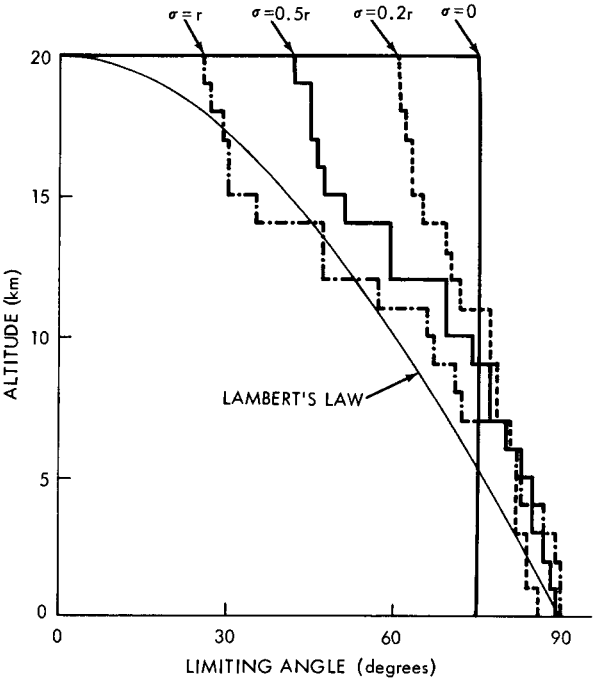

Figure 7—Statistically derived scattering characteristics.

PROPOSED SATELLITE DESIGN

The overall shape of a satellite with Lambertian surface cannot be a sensitive factor in the scattering cross section. Therefore, an erection technique should be considered which does not require gas pressurization of the entire volume or a leak-proof outer skin. Instead, only a framework of beams which form the edges of a polyhedron must be erected by gas pressure, and the skin can be lightened by using thinner, perforated sheets. With sufficiently small holes, no transparency or other losses will result up to microwave frequencies; however, the solar radiation pressure will be reduced.

Regular polyhedrons with parallel pairs of faces have an interesting property. If their surfaces obey Lambert's law, the monostatic scattering cross section becomes independent of the angular orientation, whereas the bistatic scattering cross section shows minor fluctuations which decrease as the number of faces increases. It is quite easy to derive this scattering cross section for the simplest polyhedron of this group, the cube. In Figure 8 the cube is shown in a special orientation, in which one pair of faces is parallel to the plane formed by the transmitter T, the receiver R, and the cube. The cube is rotated so that one face forms the angle ϕ with the direction of the transmitter. The bistatic angle is ψ and the side of the cube d. Hence, the powers intercepted by the two illuminated faces are

$$\left.\begin{aligned} P_1 &= Hd^2 \cos\phi \ , \\ P_2 &= Hd^2 \sin\phi \ . \end{aligned}\right\} \quad (10)$$

Lambertian scattering results in circular beam patterns; consequently, the peak values of the radiant intensities become

$$\left.\begin{aligned} J_{1m} &= \frac{aP_1}{\pi} \ , \\ J_{2m} &= \frac{aP_2}{\pi} \ . \end{aligned}\right\} \quad (11)$$

Thus, the intensity in the arbitrary direction ψ becomes

$$J_\psi = J_1 + J_2 = J_{1m} \cos\omega_1 + J_{2m} \cos\omega_2 \ . \quad (12)$$

From the expressions of Equations 10 and 11 and the angular relations of Figure 8, we derive

$$J_\psi = \frac{ad^2H}{\pi}\left[\cos\phi\cos(\phi+\psi) + \sin\phi\cos\left(\frac{\pi}{2}-\phi-\psi\right)\right],$$

$$J_\psi = \frac{ad^2H}{\pi}\cos\psi \ . \quad (13)$$

Equation 13 describes the Lambertian characteristic for a plane surface of the area d^2 normal to the incident radiation.

The rotation of the cube seems to have no effect. This, however, is not true because Lambert's law is restricted to a single lobe of

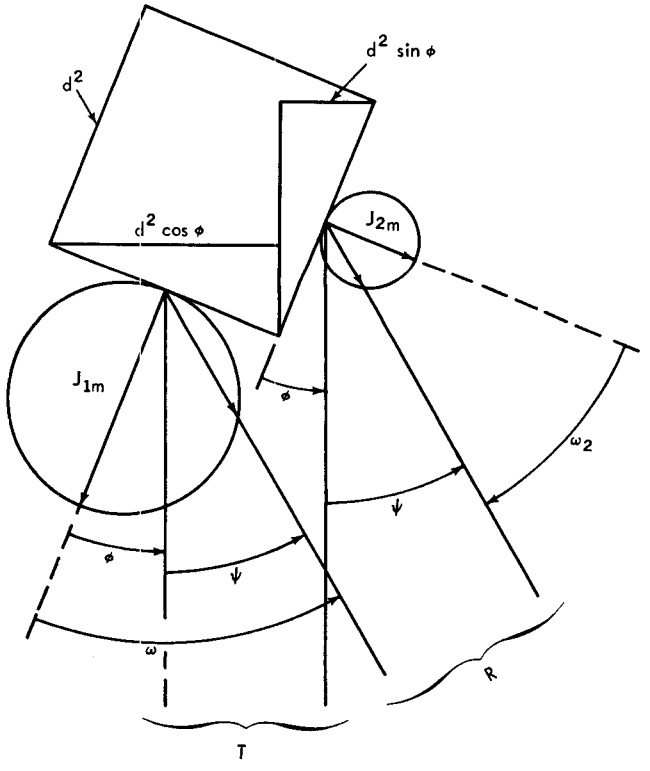

Figure 8—Lambertian scattering from two faces of a cube.

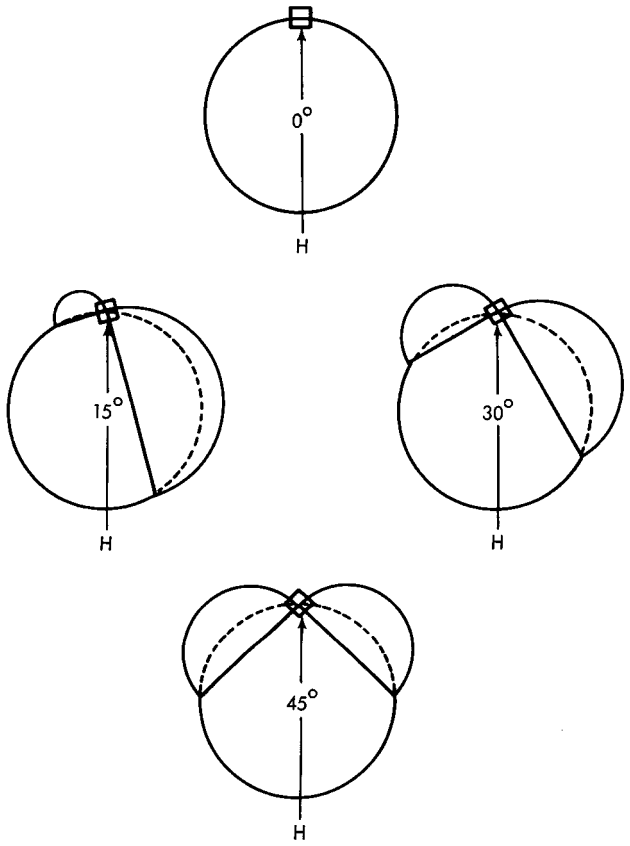

Figure 9—Lambertian scattering patterns of a cube in various angular positions.

the cosine pattern, which means that in Equation 12 ω_1 and ω_2 may only take values for which their cosines are positive. Consequently, the patterns take the forms of those shown (Figure 9) for various angular orientations of the cube, and we can see that the monostatic cross section remains unaffected by rotation.

Since the pattern of a spherical satellite was shown to be particularly useful and since the frequency diversity technique requires scattering centers at various depths, a polyhedron with a large number of faces is preferable. A small model (1.83 m diameter) of the inscribed sphere was built and tested for the National Aeronautics and Space Administration.* A regular dodecahedron was chosen for the completed model (Figure 10). The model was erected from a small, randomly compacted package by inflating the tubular framework; the skin, a perforated aluminum-polyester laminate, developed wrinkles automatically. However, one of the pentagons was covered with unperforated, wrinkled aluminum foil. Seven adjacent pentagons were covered with a skin which was only 16.5 percent larger than the pentagon in linear dimensions, and five were covered with a 45 percent larger skin so that deeper wrinkles could form.

Designs and computations of full-size satellites have been prepared for the U. S. Navy by General Mills, Inc. (Reference 3). Of particular interest are the weight savings afforded by the diffusely scattering satellite over the specularly reflecting sphere. These savings increase with the size of the satellites. In other words, more signal strength per unit weight of the satellite can be obtained from diffusely reflecting satellites supported by a tubular framework. For example, a 200-lb, diffusely scattering sphere has a diameter of 165 feet, while the specularly reflecting sphere has a diameter of 105 feet, or even less. This means an increase of the intercepting cross section by a factor of 2.5, or 4 db. If we add the gain of 3 db due to the directivity of the scattered radiation from a diffuse satellite, the total gain becomes 7 db for the Lambertian satellite of near spherical shape.

Greater reliability and longer life can also be expected from the diffusely scattering satellite. The erection by inflation of the tubular framework can be controlled better than the inflation of a large balloon in space and a random surface within wide tolerances is easier achieved and maintained than a precise spherical surface.

*Contracts NAS 5-890 and NAS 5-1598.

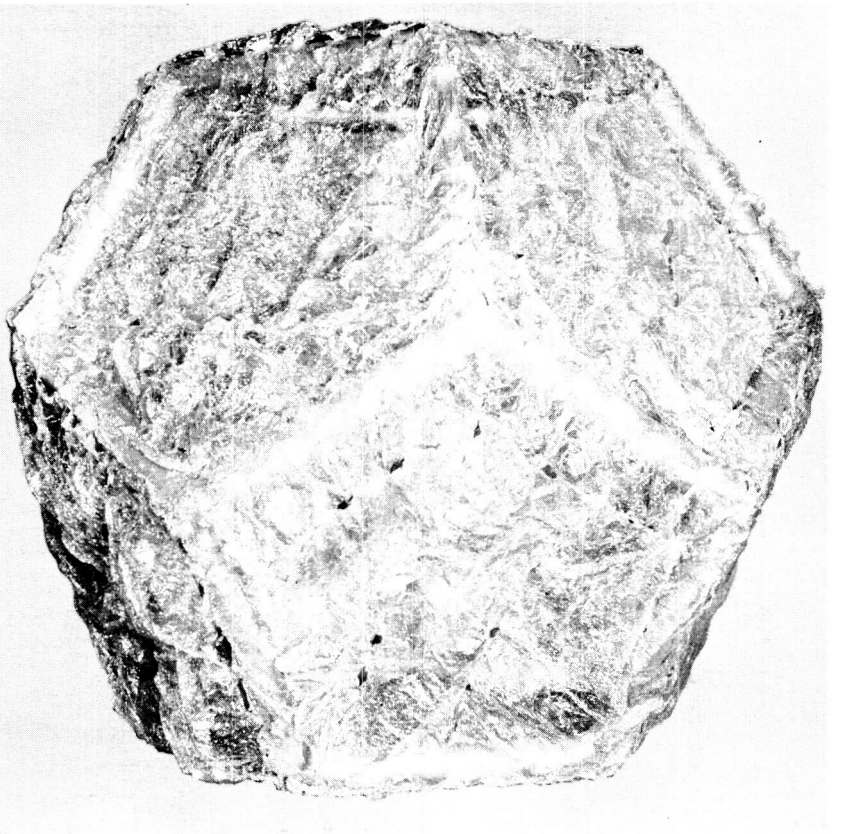

Figure 10—Satellite model with Lambertian surface.

ELECTROMAGNETIC TEST RESULTS

Measurements of monostatic and 90-degree bistatic scattering cross sections were performed by Radiation, Inc. on an outdoor range at a radio frequency of 10 Gc. The wavelength of 3 cm is about ten times too long to give realistic scaling with respect to the size of the model. However, if the cross section is at a level to confirm Lambertian scattering, it will stay that high for all higher frequencies, provided the perforation of the skin is small enough. During the tests, the model was rotated and tilted to give readings for all possible aspects. A typical recording of the cross section as the model revolved 16 degrees is presented in Figure 11. The recording is that of a stationary time series; therefore, statistical parameters were evaluated from the entire portion of the recording. Fluctuations extend over a wide range and, owing to the logarithmic scale, depressions are overemphasized. The probability distribution function and the probability density function derived by graphic means and shown in Figures 12 and 13 display good agreement with theoretical exponential distribution. The latter has been added to the figures with parameters chosen for the best fit. Since the probability density function as the derivative of the distribution function is very sensitive to errors in the evaluation process, some of the deviations of the density function from the experimental law may be discounted as errors.

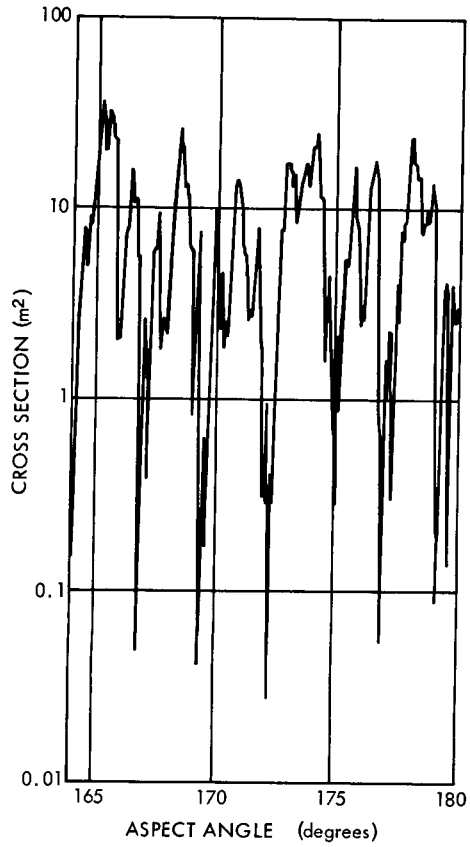

Figure 11—Section of the recording of the monostatic scattering cross section.

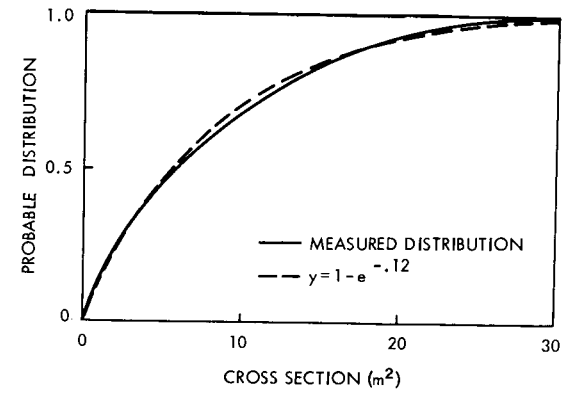

Figure 12—Probability distribution function of the monostatic scattering cross section of the satellite model.

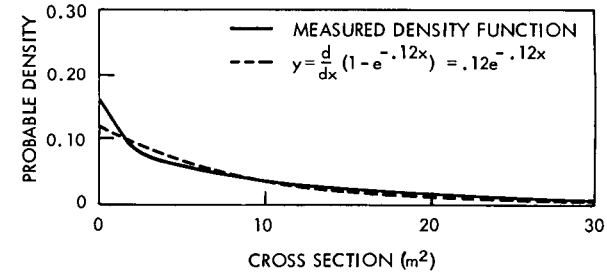

Figure 13—Probability density function of the monostatic scattering cross section of the satellite model.

The recording (Figure 11) was calibrated by means of a flat disk of known cross section. Thus we obtained a median level of 7.1 m^2 and a mean of 10.2 m^2 and derived a monostatic gain of 4.8 db over the scattering cross section of a specularly reflecting sphere with the same physical cross section as that of the model. Theoretically, the gain of a Lambertian sphere would be 4.3 db.

The entire monostatic recording showed variations of statistical parameters. Evaluation of other portions which appeared stationary in time revealed many areas where the gain was higher, for example, 5 db over a 60 degree portion, 6.5 db over a 36 degree portion, and as much as 8.3 db over a 25 degree portion. Smaller portions showed less gain. The lowest gain was 1.9 db over a 20 degree portion. Some of these deviations could be explained: For example, the highest gain was noted when the lightly wrinkled aluminum foil face was in a position normal to the transmission path. It did not diffuse the radiation sufficiently and thus contributed to the lowest gain when the foil was tilted but still on the illuminated side of the model. When the deeply wrinkled faces were on the illuminated side, the return was so stationary that a periodicity due to symmetries of the model could not be observed.

The generally higher gain of the model than that of a Lambertian sphere is due to the polyhedral shape. For example, a cube (which deviates even more from a sphere) has a theoretical gain

of 6 db. As a consequence, the bistatic scattering cross section was in average 4.5 db lower than that of a Lambertian sphere.

The fluctuation of the cross section shown in Figure 11 was the slowest recorded and agrees well with the expected rate because of the rotational rate, wavelength, and size of the model. Other portions of the recording showed considerably faster fluctuation. This fluctuation rate can be explained as a wind effect, since even the slight breeze observed caused the light and unsupported skin to wave. To test this explanation, the rotation of the model was stopped on one occasion; and, as the recorder continued, the distribution and fluctuation rate of the cross section remained unchanged.

Because of the wind, it was not possible to obtain the cross section-versus-frequency data necessary to determine the spacing for frequency diversity. The amount of depolarization was determined by rotating the polarization of the transmitting antenna 90 degrees. It was found that the cross-polarized echo was 6 db lower than the return of paralled polarization.

CONCLUSION

A passive communication satellite consisting of a tubular framework and a randomly wrinkled, perforated, and reflective skin will scatter electromagnetic waves according to Lambert's law. Consequently, a scattering pattern of very suitable directivity can be gained with a device which is lighter and more reliable than a specularly reflecting sphere. The Rayleigh distribtuion of the return requires the use of diversity techniques, whereby the frequency diversity is most attractive and can be realized with no additional power or antenna requirements.

REFERENCES

1. Kahn, L. R., "Ratio Squarer," *Proc. IRE* 42(11):1704, November 1954.

2. Brennan, D. G., "On the Maximum Signal-to-Noise Ratio Realizable from Several Noisy Signals," *Proc. IRE* 43(10):1530, October 1955.

3. "Large Passive Satellite Study," Vol. I and II. Final report on Contract Nonr (3245)(00)(X).